Impact of Wavelength-Dependent I/Q Imbalances of Standard C-Band Transceivers in Rate-Adaptive Multiband Systems

Gabriele Di Rosa(1), Robert Emmerich(2), Matheus Sena(2), Johannes K. Fischer(2), Colja Schubert(2), André Richter (1)

(1) VPIphotonics GmbH, Carnotstr. 6, Berlin, Germany, gabriele.di.rosa@vpiphotonics.com
(2) Fraunhofer Institute for Telecommunications, Heinrich-Hertz-Institute, Einsteinufer 37, Berlin, Germany

Abstract *We experimentally characterize wavelength-dependent I/Q imbalances when operating standard C-band IQ-modulator and coherent receiver in S-C-L-band systems. We evaluate their impact on the achievable entropy rate for probabilistically shaped PDM-256/64-QAM and show no penalty up to 150 nm bandwidth based on a single calibration.*

Introduction

The constant growth in IP traffic is fostering, together with the need for operators to maximize the exploitation of the existing fiber infrastructure, the rapid deployment of multiband (MB) wavelength division multiplexing (WDM) systems. This solution represents a cost-effective approach to increase the channel capacity[1], in particular combined with spectrally efficient higher-order modulation formats. With the currently available technology, a bandwidth of up to 150 nm has been experimentally demonstrated for polarization division multiplexed (PDM) 64 GBd 64-QAM employing standard C-band off-the-shelf components and commercial doped fiber amplifiers[2],[3]. At the same time, extensive research is being carried out to maximize the overall performance over the fiber optic channel for S-C-L-band systems. In this context, seamless MB amplification schemes[4] and advanced power optimization strategies[5]–[7] have been proposed. Furthermore, recent record experiments have pointed out the advantages of employing rate-adaptivity through constellation shaping to maximize the fiber channel capacity over the wavelength-dependent end-to-end channel[8]. However, this approach poses severe requirements on the transceivers, which have to provide higher-order base constellations. With commercial solutions for the S-band being not yet available, the only logical option is to use standard C-band transceivers over the whole wavelength range. In this scenario, it is crucial to investigate the I/Q imbalances of transceivers working outside their operative wavelength range to understand system limitations[9].

In this contribution, we experimentally characterize the wavelength-dependent I/Q imbalances for off-the-shelf C-band transceivers working in S-C-L-band systems. This operation is performed by separately monitoring transmitter (Tx) and receiver (Rx) I/Q amplitude and phase imbalance and I/Q skew through receiver-side digital signal processing (DSP) applied on back-to-back transmission data[10]. Nonlinear transmitter predistortion based on system identification[11] is performed only once at 1500 nm to derive an ideal waveform, and calibration of the coherent receiver skew inside the scope was performed only at 1550 nm for optimal C-band performance. Subsequently, we simulate the impact of I/Q imbalances on the achievable entropy of rate-adaptive MB systems employing probabilistic shaping (PS). We determine that in the experimentally observed range of imbalances a penalty-free operation over the whole considered bandwidth is guaranteed with a large margin.

Experimental setup

The experimental setup used for the characterization of the wavelength-dependent I/Q imbalances is provided in Fig. 1. The predistorted signal for all three bands is generated using a single commercially available C-band $LiNbO_3$ dual polarization IQ modulator. External cavity lasers are optically amplified for the S+L-band to the same power as the C-Band laser (16 dBm) in front of the modulator. The electrical signal to drive the modulator is generated from a 120 GSa/s, 8-bit, 4 channel DAC. The obtained and optimized Tx 32-QAM 64 GBd waveforms are based on system identification[11] applied to the S-band[2]

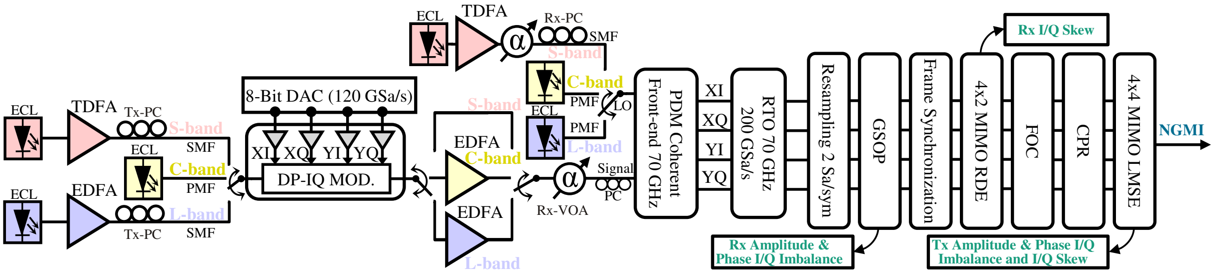

Fig. 1: Experimental setup used for MB back-to-back transmission with intradyne coherent reception including offline DSP for I/Q imbalance characterization of C-Band transceivers. ECL: External Cavity Laser. EDFA: Erbium Doped Fiber Amplifier. TDFA: Thulium Doped Fiber Amplifier. PC: Polarization Controller. PMF: Polarization Maintaining Fiber. SMF: Single Mode Fiber. DAC: Digital to Analog Converter. VOA: Variable Optical Attenuator. RTO: Real Time Oscilloscope.

at 1500 nm. The achieved optical power in the S-band is wavelength-dependent and varies between -5.2 and -8 dBm as described in detail in[12]. At the receiver, per band amplification for the C-L-band is used while the S-band is not amplified. Selection of the band is performed using a switch before and after the modulator. A variable optical attenuator is used in front of the Rx to optimize the signal power into the coherent receiver front-end (CRF). The signal is mixed with the local oscillator (LO) in the 70 GHz CRF comprising an optical free-space based C-band dual polarization 90°-Hybrid. For the C-L-band, a laser at 14 dBm is used while for the S-band a low power laser is amplified as LO to perform intradyne coherent reception in all bands. The outputs of the CRF are subsequently digitized at a sampling rate of 200 GSa/s using a 4-channel RTO with 70 GHz analog electrical bandwidth and 8-bit resolution.

I/Q imbalances characterization

I/Q imbalances due to Tx and Rx imperfections can be separately evaluated in the presence of frequency offset (FO) through the receiver-side DSP[10]. In particular, Rx amplitude and phase imbalances can be estimated by the Gram-Schmidt orthonormalization procedure (GSOP) while Rx skew can be monitored through the converged taps of the 25-tap 4x2 multiple-input multiple-output (MIMO) radius directed equalizer (RDE)[13], which operates at 2 samples/symbol. Similarly, Tx impairments can be estimated in the 4x4 MIMO post-equalizer[14]. For this purpose, a symbol-spaced 1-tap least-mean squares equalizer (LMSE) is used to monitor amplitude and phase imbalance, while 35 taps are used for the skew. To ensure maximum accuracy for the estimation, all the equalizers and the carrier phase recovery (CPR) operate in a fully-data-aided mode. Synchronization and frequency offset compensation (FOC) are instead based on a training sequence of 448 symbols periodically

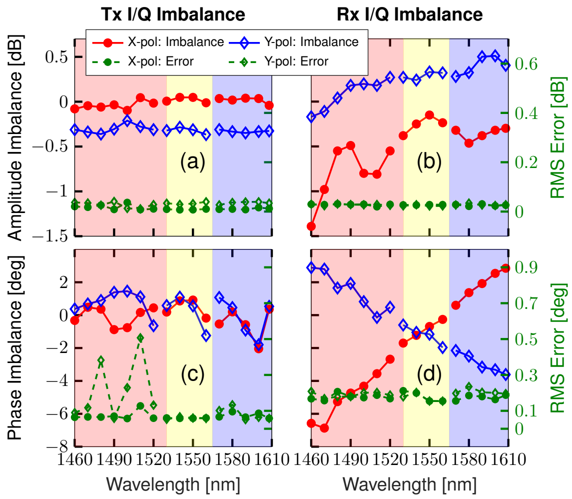

Fig. 2: Estimated Tx and Rx I/Q imbalances and error of the method: (a) Tx amplitude imbalance, (b) Rx amplitude imbalance, (c) Tx phase imbalance, (d) Rx phase imbalance.

transmitted every 2^{15} symbols.

The results of the characterization are visualized in Fig. 2, where the estimated I/Q imbalances, defined as in[10], and the root mean square (RMS) error of the estimation method are shown. To evaluate the RMS error, a simulation setup in VPIphotonics Design Suite 11.1 comprising of transceivers with tunable I/Q imbalances and additive white Gaussian noise (AWGN) loading is implemented. For each wavelength, 50 different simulations with random noise realization and transmitted sequence are performed. The I/Q imbalances are set in each case to the characterized values, including the monitored Tx/Rx I/Q skews. Skews are given by imperfections in the electrical subsystems and, as expected, are found to be wavelength-independent and are then not discussed further. The skew monitoring and correction is performed in any case to avoid impacting the accuracy of the other monitors[10]. To fairly assess the error of the method, the received SNR in the simulations is set to the values observed in the experiment, ranging from 18 to 22 dB. From Fig. 2, we see that the RMS error is in most cases negligible, with spikes for the Tx phase imbalance monitor at some wavelengths for which only a small FO < 5 MHz was measured. These are evident in the Y polarization, due to the larger Tx amplitude imbalance, but they do not hinder the conclusions of our analysis. From Fig. 2(a,c) we observe in fact that Tx I/Q imbalances are practically wavelength-independent. For the amplitude (Fig. 2(a)), we observe an almost perfect balance in the X polarization while the Y polarization shows minimum imbalance at 1500 nm, where the predistortion was performed, and an almost wavelength-independent behavior moving away from 1500 nm, with a maximum value of ≈ 0.4 dB. At the same time, the phase imbalance (Fig. 2 (c)) remains inside a small range of $\pm 2°$. On the contrary, Rx imbalances show a clear wavelength dependency, as visible in Fig. 2(b,d)). While in C-band we observe maximum absolute values of respectively ≈ 0.4 dB and $\approx 2°$ for amplitude and phase imbalance, these values grow to ≈ 1.4 dB and $\approx 7°$ at 1460 nm. The phase imbalance, in particular, shows a linear growth moving outside the C-band. This behavior may suggest that the linear wavelength dependency of phase shifters inside the optical dual polarization $90°$-Hybrid is dominating the characterized phase imbalance[15].

Impact of I/Q imbalances on maximum signal entropy

To assess the impact of the wavelength-dependent I/Q imbalances on the achievable signal entropy, we perform simulations for 256/64-QAM-PS over an AWGN channel with a received SNR of 20 dB and 15 dB, respectively. The laser linewidth of Tx laser and LO are set to 100 kHz as in the experiment, the FO to 100 MHz, and a realistic format-independent pilot-based DSP is implemented in place of the fully-data-aided algorithms used during the characterization. QPSK pilots are inserted in the transmitted sequence at a rate of $1/32$ and a header of 512 symbols is introduced at the start of the 2^{17} symbols frame, leading to a pilot overhead $\approx 3.51\%$. The pilots are used for the equalizers update and to perform CPR. The payload symbols are drawn from the Maxwell-Boltzmann distribution to achieve a target entropy, which is swept to find the maximum value for which the normalized generalized mutual information (NGMI), calculated on the received signal as in[16], is > 0.88. The results of this study are shown in Fig. 3, where the Tx imbalances are swept either assuming an ideal Rx, or with Rx imbalances much larger than the maximum values characterized during the experiment. This analysis is carried out to show that Rx imbalances are effectively removed by the GSOP and do not affect the performance. On the contrary, Tx-side imperfections are mitigated only at the end of the DSP chain and have a detrimental impact, thus reducing the maximum source information rate for post-FEC error-free operation. However, focusing on the experimentally observed range of Tx imbalances (the area in red in Fig. 3) we can observe that practically penalty-free operation is preserved with a large margin in all the conditions considered.

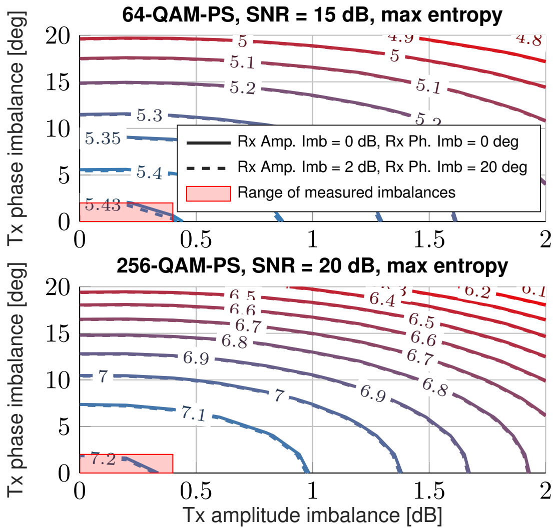

Fig. 3: Achievable signal entropy versus transceiver I/Q imbalances.

Conclusions

We experimentally characterized the wavelength-dependency of I/Q imbalances for a system employing off-the-shelf C-band transceivers in S-C-L-band systems. While the receiver shows an evident wavelength dependency, the transmitter demonstrated very limited I/Q imbalances over 150 nm bandwidth by using a one-time calibrated predistortion. This behavior, combined with the effectiveness of standard receiver front-end correction DSP in mitigating receiver imbalances, allowed to observe through additional simulations no penalty in the maximum transmitted signal entropy with a large margin for 256/64-QAM-PS.

Acknowledgements

This work is funded by the EU under H2020-MSCA-ITN-2018 Grant Agreement 814276 (WON) and the German Federal Ministry of Education and Research under the grant 16KIS0993 and 16KIS0990 (OptiCON).

References

[1] A. Ferrari, A. Napoli, J. K. Fischer, N. Costa, A. D'Amico, J. Pedro, W. Forysiak, E. Pincemin, A. Lord, A. Stavdas, *et al.*, "Assessment on the achievable throughput of multi-band ITU-T G. 652. D fiber transmission systems", *Journal of Lightwave Technology*, vol. 38, no. 16, pp. 4279–4291, 2020.

[2] R. Emmerich, M. Sena, R. Elschner, C. Schmidt-Langhorst, I. Sackey, C. Schubert, and R. Freund, "Enabling S-C-L-band systems with standard C-band modulator and coherent receiver using nonlinear predistortion", in *Optical Fiber Conference (OFC)*, paper F4D.7, 2021, pp. 1–3.

[3] M. Sena, R. Emmerich, B. Shariati, J. K. Fischer, and R. Freund, "Evaluation of an autonomous digital predistortion scheme for optical multiband systems", in *Optical Fiber Conference (OFC)*, paper F4D.5, 2021, pp. 1–3.

[4] M. A. Iqbal, L. Krzczanowicz, I. Phillips, P. Harper, and W. Forysiak, "150nm SCL-band transmission through 70km SMF using ultra-wideband dual-stage discrete raman amplifier", in *2020 Optical Fiber Communications Conference and Exhibition (OFC)*, 2020, pp. 1–3.

[5] D. Uzunidis, C. Matrakidis, A. Stavdas, and A. Lord, "Power optimization strategy for multi-band optical systems", in *2020 European Conference on Optical Communications (ECOC)*, 2020, pp. 1–4. DOI: 10.1109/ECOC48923.2020.9333398.

[6] F. Hamaoka, M. Nakamura, S. Okamoto, K. Minoguchi, T. Sasai, A. Matsushita, E. Yamazaki, and Y. Kisaka, "Ultra-wideband WDM transmission in S-, C-, and L-bands using signal power optimization scheme", *Journal of Lightwave Technology*, vol. 37, no. 8, pp. 1764–1771, 2019. DOI: 10.1109/JLT.2019.2894827.

[7] B. Correia, R. Sadeghi, E. Virgillito, A. Napoli, N. Costa, J. Pedro, and V. Curri, "Power control strategies and network performance assessment for C+L+S multiband optical transport", *J. Opt. Commun. Netw.*, vol. 13, no. 7, pp. 147–157, Jul. 2021. DOI: 10.1364/JOCN.419293. [Online]. Available: http://jocn.osa.org/abstract.cfm?URI=jocn-13-7-147.

[8] L. Galdino, A. Edwards, W. Yi, E. Sillekens, Y. Wakayama, T. Gerard, W. S. Pelouch, S. Barnes, T. Tsuritani, R. I. Killey, D. Lavery, and P. Bayvel, "Optical fibre capacity optimisation via continuous bandwidth amplification and geometric shaping", *IEEE Photonics Technology Letters*, vol. 32, no. 17, pp. 1021–1024, 2020. DOI: 10.1109/LPT.2020.3007591.

[9] M. Sena, Y. Cui, G. Fiol, B. Shariati, A. Napoli, J. K. Fischer, M. Schell, and R. Freund, "Performance evaluation of InP-based DP-IQ modulators for multiband transmission systems", in *2020 22nd International Conference on Transparent Optical Networks (ICTON)*, 2020, pp. 1–4. DOI: 10.1109/ICTON51198.2020.9203554.

[10] J. Liang, Y. Fan, Z. Tao, X. Su, and H. Nakashima, "Transceiver imbalances compensation and monitoring by receiver DSP", *Journal of Lightwave Technology*, pp. 1–1, 2019. DOI: 10.1109/JLT.2019.2944830.

[11] M. Nölle, M. S. Erkilinç, R. Emmerich, C. Schmidt-Langhorst, R. Elschner, and C. Schubert, "Characterization and linearization of high bandwidth integrated optical transmitter modules", in *2020 European Conference on Optical Communications (ECOC)*, paper Tu2D-4, 2020, pp. 1–4. DOI: 10.1109/ECOC48923.2020.9333184.

[12] R. Emmerich, M. Sena, M. S. Erkilinç, I. Sackey, R. Elschner, C. Schmidt-Langhorst, C. Schubert, and R. Freund, "S-band transmission with off-the-shelf C-band components enabled by nonlinear predistortion based on coherent system identification", in *Proc. of Photonic Networks; 22th ITG Symposium, Online*, ITG-Fb. 297: Photonische Netze, May 2021, pp. 77–83.

[13] R. Rios-Müller, J. Renaudier, and G. Charlet, "Blind receiver skew compensation and estimation for long-haul non-dispersion managed systems using adaptive equalizer", *Journal of Lightwave Technology*, vol. 33, no. 7, pp. 1315–1318, 2015.

[14] C. R. S. Fludger and T. Kupfer, "Transmitter impairment mitigation and monitoring for high baud-rate, high order modulation systems", in *ECOC 2016; 42nd European Conference on Optical Communication*, 2016, pp. 1–3.

[15] Y. Nasu, T. Mizuno, R. Kasahara, and T. Saida, "Temperature insensitive and ultra wideband silica-based dual polarization optical hybrid for coherent receiver with highly symmetrical interferometer design", *Optics express*, vol. 19, no. 26, B112–B118, 2011.

[16] J. Cho, L. Schmalen, and P. J. Winzer, "Normalized generalized mutual information as a forward error correction threshold for probabilistically shaped QAM", in *2017 European Conference on Optical Communication (ECOC)*, paper M.2.D.2, 2017, pp. 1–3. DOI: 10.1109/ECOC.2017.8345872.